CO2 isolated line shapes by classical molecular dynamics simulations: Influence of the intermolecular potential and comparison with new measurements

G. Larcher, H. Tran, M. Schwell, P. Chelin, X. Landsheere, J.-M. Hartmann, and S.-M. Hu

---

Articles you may be interested in

CO₂ isolated line shapes by classical molecular dynamics simulations: Influence of the intermolecular potential and comparison with new measurements

G. Larcher,[1] H. Tran,[1,a)] M. Schwell,[1] P. Chelin,[1] X. Landsheere,[1] J.-M. Hartmann,[1] and S.-M. Hu[2]

[1]*Laboratoire Interuniversitaire des Systèmes Atmosphériques (LISA, CNRS UMR 7583), Université Paris Est Créteil, Université Paris Diderot, Institut Pierre-Simon Laplace, 94010 Créteil Cedex, France*
[2]*Hefei National Laboratory for Sciences at Microscale, University of Science and Technology of China, 230026 Hefei, China*

Room temperature absorption spectra of various transitions of pure CO_2 have been measured in a broad pressure range using a tunable diode-laser and a cavity ring-down spectrometer, respectively, in the 1.6 μm and 0.8 μm regions. Their spectral shapes have been calculated by requantized classical molecular dynamics simulations. From the time-dependent auto-correlation function of the molecular dipole, including Doppler and collisional effects, spectral shapes are directly computed without the use of any adjusted parameter. Analysis of the spectra calculated using three different anisotropic intermolecular potentials shows that the shapes of pure CO_2 lines, in terms of both the Lorentz widths and non-Voigt effects, slightly depend on the used potential. Comparisons between these *ab initio* calculations and the measured spectra show satisfactory agreement for all considered transitions (from J = 6 to J = 46). They also show that non-Voigt effects on the shape of CO_2 transitions are almost independent of the rotational quantum number of the considered lines. © *2014 AIP Publishing LLC*. [http://dx.doi.org/10.1063/1.4866449]

I. INTRODUCTION

Classical molecular dynamics simulations (CMDS) have recently been successfully used to predict different physical properties related to intermolecular interactions (e.g., Refs. 1–4). For CO_2, they have been used to calculate the spectral shape of the far wings of infrared and Rayleigh scattering bands[2,5] and of the far infrared collision-induced absorption band.[3] In a recent study,[6] we have shown that using an appropriate requantization procedure for molecular rotations in CMDS, we were able to predict the spectral shape of CO_2 isolated transitions. This was made using an anisotropic intermolecular potential[7] to represent the interactions between molecules. Requantized classical molecular dynamics simulations (rCMDS) provided the time-dependent dipole auto-correlation function whose Fourier-Laplace transform directly yields the spectral shape. Comparisons between these *ab initio* calculations with absorption lines measured in different bands of CO_2 for a limited set of rotational quantum numbers J (J = 12–16) showed very good agreement.[6]

These calculations are extended in the present work to a wider range of the rotational quantum number J. For that, new spectra of CO_2 have been measured at room temperature and for many pressures using an external-cavity diode laser system in the 1.6 μm region. Spectra recorded by a cavity ring-down spectrometer system in the 0.8 μm region[8] are also used. These spectra, measured in two different spectral regions, for large ranges of pressure (i.e., from 0.003 to 1 atm) and many rotational quantum numbers (from J = 6 to J = 46) thus enable meaningful tests of the rCMDS calculations. Furthermore, the influence of the intermolecular potential on the line shape is also investigated by using three different anisotropic potential energy surfaces (PES)[7,9,10] in the calculations. Comparisons between the diffusion coefficients, the Lorentz widths and the line shapes obtained with these PESs are made. The results show that these quantities slightly depend on the potential, in contrast with the case of the far infrared collision-induced absorption band.[3,11] Comparisons between rCMDS calculations and measured spectra show satisfactory agreement for all considered lines. They also show that non-Voigt effects on the line shape of CO_2 are almost independent of the rotational quantum number of the considered line.

This paper is organized as follows. Section II summarizes the experimental set-up and the measurement procedure. The rCMDS calculations and the potentials used are described in Sec. III. Comparisons between rCMDS results and measurements are presented and discussed in Sec. IV. Conclusions and future studies are drawn in Sec. V.

II. EXPERIMENTAL SET-UP AND MEASUREMENT PROCEDURE

A. Tunable diode laser spectroscopy (TDLS)

The experimental set-up, presented in Figure 1, is mostly based on the one described in Refs. 12 and 13 that was used to measure spectra of water around 0.8 μm. The experimental spectra presented in this work have been recorded using

---

a)Author to whom correspondence should be addressed. Electronic mail: ha.tran@lisa.u-pec.fr
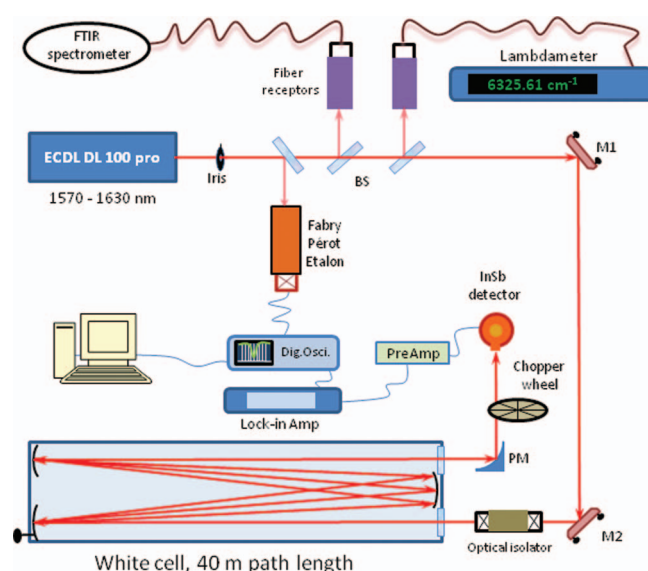
FIG. 1. The experimental setup used at LISA. BS: beamsplitters, M1, M2: plane mirrors, PM: parabolic mirror.

an external-cavity diode laser (ECDL) (Toptica Photonics, DL100 pro design) operating in the 6100–6400 cm^{-1} spectral range with a mode-hop free tuning range broader than 30 GHz (1 cm^{-1}). This laser is equipped with a beam steering mirror compensating for beam displacements while scanning. Its stated emission line width, of about 1 MHz (0.000033 cm^{-1}) or better, is negligible with respect to the room temperature Doppler width of CO_2 lines in this spectral region (about 0.0058 cm^{-1}). We have checked the ECDL output purity with a FTIR spectrometer (Bruker IFS 125-HR) at 0.002 cm^{-1} spectral resolution and also a laser spectrum analyzer (Bristol 721A NIR). No residual spontaneous emission of the ECDL has been detected. In order to prevent interference effects between optical elements and the diode-laser cavity, two optical isolators of 35 dB and 60 dB, respectively, are used too. The first one (Toptica 35 dB) is integrated inside the laser head and the second one (Thorlabs 60 dB) is placed right in front of the entrance window of the absorption cell. The laser beam is directed into a White-type multipass absorption cell (1 m base length, maximum pathlength 40 m). The light transmitted by the cell is focalized onto a liquid-nitrogen-cooled InSb diode detector (EG and G Judson J10D) connected to a low-noise pre-amplifier.

One scan cycle of about 1 cm^{-1} takes approximately 10 s and typically 20 of these cycles are averaged to obtain an absorption spectrum. Cares have been made in order to ensure that only cycles without notable laser instability are taken into account in the averaging procedure. A mechanical chopper (Scitec Instruments) is used to modulate the signal from the InSb detector at about 3 kHz and the latter is then de-modulated and amplified using a digital lock-in amplifier (Perkin Elmer DSP 7265). The output signal of the lock-in amplifier is recorded using a LabView driven acquisition card (National Instruments NI-6123) at a rate of 2000 points/s and with a resolution of 16 bits. Note that the time constant of the lock-in amplifier, which denotes the integration time of the signal, is kept below 5 ms. This is necessary in order not to

distort the shape of absorption lines studied. In parallel, the Fabry-Perot etalon signal (with free spectral range of 1 GHz) is recorded and digitized. Its series of narrow peaks are used to construct the relative wavenumber scale as described in detail in Ref. 12. Briefly, each etalon peak is fitted by a Gaussian profile, and the peak positions in time are converted to relative wavenumbers using a third degree polynomial function in order to account for the slight non-linearity of the ECDL tuning.

All pressures were measured using two capacitive pressure transducers (MKS Baratron 627B) of 100 and 1000 Torr full scale with a stated accuracy of ±0.12%. The experiments were carried out as follows: a spectrum was first recorded with an empty cell, providing the 100% transmission reference. Then, pure CO_2 is injected into the cell at a pressure from 2 to 700 Torr and a self-broadened spectrum was recorded. Eleven isolated lines [R(6), R(10), R(12), R(14), R(20), R(24), R(30), R(34), P(38), R(42), P(46)] belonging to the (30013 ← 00001) or (30012 ← 00001) bands of CO_2 were investigated. Absolute frequency positions of the CO_2 lines are taken from Ref. 14 in order to determine the Doppler width for each considered line.

B. High sensitivity CRDS spectra

Various transitions of the (10052 ← 00001) band of pure CO_2 were measured using a continuous wave cavity ring-down spectrometer (cw-CRDS)[8] for pressures from 50 to 300 Torr (step of 50 Torr). The gas pressure was measured by a capacitance gauge (MKS Baratron 627B) of 1000 Torr full scale with a stated accuracy of 0.12%. The spectra were recorded at room temperature (296 ± 1 K). Typical sensitivity of the CRDS measurements, expressed with the minimal detectable absorption coefficient, was 1 × 10^{-10} cm^{-1}. The spectra were calibrated by using the longitudinal modes of a Fabry-Perot interferometer (FPI) made of ultra-low-expansion glass. The 10 cm long FPI is placed in a vacuum chamber and thermo-stabilized. The frequency fluctuation of its longitudinal modes is considerably reduced and the absolute frequencies are calibrated with an accuracy of 0.1–0.6 MHz using the atomic transitions of ^{87}Rb at 780 nm and 795 nm.[15] The CO_2 spectra have been calibrated with an accuracy of 0.7 MHz (2 × 10^{-5} cm^{-1}).

III. REQUANTIZED CLASSICAL MOLECULAR DYNAMICS SIMULATIONS

Requantized Classical Molecular Dynamics Simulations have been carried for a large number of CO_2 molecules. Details of the calculation procedure can be found in previous studies devoted to different CO_2-radiation interaction properties (e.g., Refs. 6 and 16–18). In the present work, three different intermolecular potentials have been used to represent interactions between molecules. The first one, PES1,[9] is empirical while the two others, PES2[7] and PES3,[10] result from *ab initio* calculations. All three were used in Ref. 3 in order to compute the far infrared collision-induced absorption band from first principles. The results showed that the predicted collision-induced absorption strongly depends on the

potential and that PES3[10] leads to the best agreement with measurements.

The computations have been performed on the IBM BLUEGENE/Q parallel computer of the French *Institut du Développement et des Ressources en Informatique Scientifique* (IDRIS). For each potential used, calculations have been made for about 16×10^6 linear and rigid CO_2 molecules. These molecules are initially randomly placed in 4096 independent cubic boxes, containing 4000 molecules each, with periodic boundary conditions. The size of each box is deduced from the perfect gas law with the temperature and pressure used in the calculation. For translational and rotational velocities, speeds verifying Boltzmann statistics have been chosen while random orientations have been imposed. The time evolution of the system is then calculated using the equations of classical mechanics: i.e., the force and torque applied to each molecule by its neighbors are computed at each time step. The translational velocity, the rotational angular momentum, and hence the position and axis orientation of the molecules are then determined at each time step. A temporization time (about 40 ps) has been observed in order to ensure that the system is completely thermalized.[19] The requantization procedure described in Ref. 6 is then applied to the rotational angular momentum of the molecules. For a molecule of rotational angular momentum ω_m we find the (even) integer J_m for which $\hbar J_m/I$, where I is the moment of inertia, is the closest to ω_m. The value of J_m determined in this way thus corresponds to the rotational quantum number of P branch lines. Note that, as mentioned in Ref. 16, this requantization is only applied when the torque due to intermolecular interactions is negligibly small so that this does not influence the evolution of the system.

The time-dependent auto-correlation functions (ACFs) of the molecular dipole is then computed by rCMDS, including the Doppler effect, as done in Ref. 6. For each potential, these ACFs have been calculated at room temperature and 0.2 atm pressure. This value of the pressure ensures that line-mixing effect near line centers[20] and neighboring lines contributions can be neglected and that the calculated lines can thus be considered as isolated. Several values of the Doppler width have been used (from 0.9×10^{-4} cm^{-1} to 0.2 cm^{-1}, which correspond to several values of the line position) providing a large range of values of the ratio Γ_L/Γ_D where Γ_L and Γ_D are, respectively, the Lorentz and Doppler widths. Furthermore, rCMDS have been also performed for temperatures between 200 and 600 K in order to calculate the self-diffusion coefficient of CO_2, which can be directly deduced from the ACF of the translational velocity.[21,22]

IV. RESULTS AND DISCUSSIONS

A. Diffusion coefficients

Figure 2 presents a comparison between the rCMDS-calculated mass-diffusion coefficient of pure CO_2 and measured values for different temperatures. Recall that the mass diffusion coefficient is directly deduced from the time constant ($\tau_{\bar{v}}$) of the decay of the translational velocity ACF, i.e., $D = \frac{\tau_{\bar{v}} k_B T}{m}$, with k_B the Boltzmann constant and m the molec-
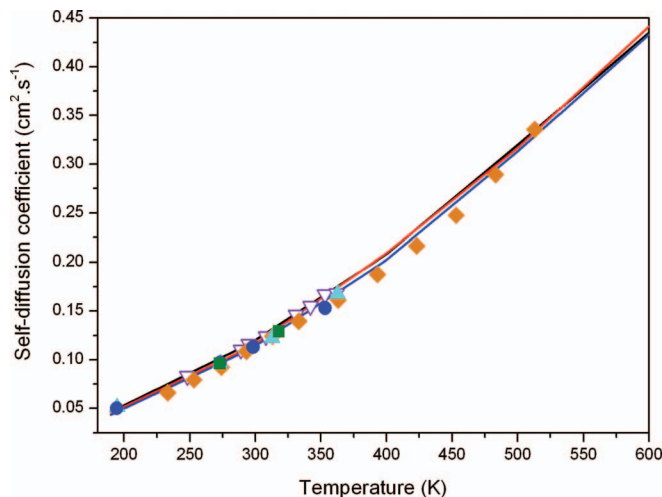

FIG. 2. Self-diffusion coefficient of CO_2 at 1 atm versus temperature calculated from rCMDS by using the potentials PES1[9] (black line), PES2[7] (red line), and PES3[10] (blue line). Measured values are from Ref. 23 (green squares), Ref. 24 (blue circles), Ref. 25 (cyan triangles), Ref. 26 (open violet triangles), and Ref. 27 (orange diamonds).

ular mass. A very good agreement can be observed as already demonstrated in Ref. 2 for a narrower temperature range. This is a first validation of the description of the molecular velocity changes by our rCMDS. The mass diffusion coefficients calculated using the three potentials are very close to each other (relative differences are smaller than 4%), somehow confirming that the diffusion of polyatomic gases is mostly governed by the isotropic part of the intermolecular interaction.

B. Lorentz line width

The theoretical absorption spectrum is directly obtained from the Fourier-Laplace transform of the dipole auto-correlation functions computed by rCMDS (see Ref. 6 for further details). From the spectrum calculated for the lowest value of the Doppler width (i.e., 0.9×10^{-4} cm^{-1}), the Lorentz broadening coefficients, γ have been obtained by fitting the rCMDS spectrum with the Voigt profile, the Doppler width being fixed. This value of the Doppler width ensures that the Dicke narrowing effect on the calculated spectrum is negligible and that line broadening is mainly due to collisions. Figure 3 shows a comparison between the values obtained with the three potentials and experimental values of Refs. 28 and 29. The latter were also obtained from fits of measured spectra using Voigt line shapes. The broadening coefficients obtained by fitting the TDLS spectra measured in this work with the Voigt profile are also reported, γ being determined as the slope of the linear fit of the Lorentz line width obtained at different pressures versus pressure. All measured values are for transitions of the (30013 ← 00001) band except for the P(38) and P(46) lines measured in the present work, which belong to the (30012 ← 00001) band.

As can be observed, the broadening coefficients measured in this work are in very good agreement with the previous experimental determinations[28,29] (within the error bars of 2%). The calculated values using PES2[7] and PES3[10] are very similar, both smaller than those obtained with PES1[9]
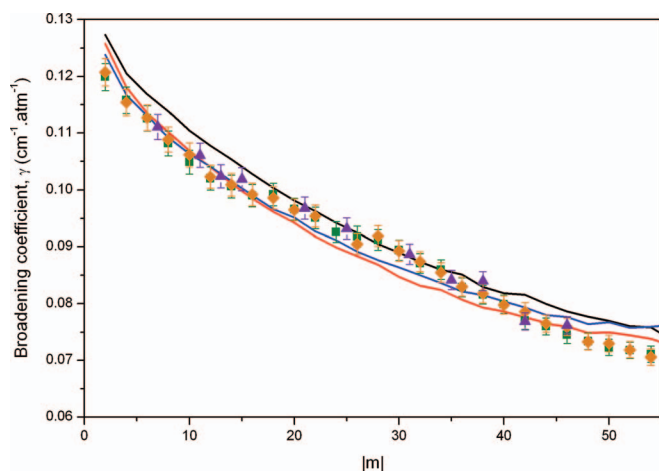
FIG. 3. Lorentz self-broadening coefficients of CO_2 versus |m| (with m = −J and m = J + 1 for P(J) and R(J) branch lines, respectively). Black, red, and blue lines are results obtained from fits with Voigt profiles of rCMDS spectra calculated with PES1,[9] PES2,[7] and PES3,[10] respectively. Symbols are values retrieved from measured spectra in Ref. 28 (orange diamonds), Ref. 29 (green rectangles), and the present work (violet triangles). Indicative error bars of ±2% have been added to the measured values.
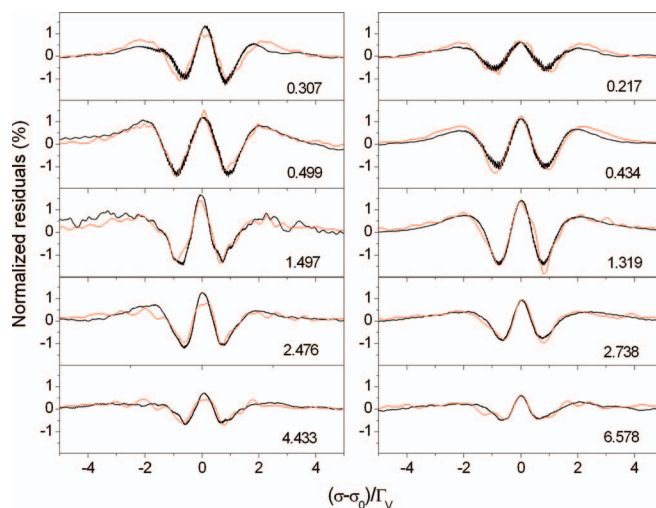

FIG. 4. Peak-absorption-normalized residuals obtained from fits with the Voigt profile of TDLS measured spectra (black lines, Sec. II A) and of rCMDS-calculated spectra (red lines) obtained by using PES3.[10] In the left and right columns are the results obtained for the R(6) and R(20) lines, the number in each panel being the corresponding Lorentz to Doppler widths (Γ_L/Γ_D) ratio.

with a maximum difference of about 5%. These two potentials also lead to results in better agreement with the measured broadening coefficients. This shows that, with respect to the mass diffusion coefficient, the line width is more sensitive to the intermolecular potential and that the empirical potential PES1[9] is not accurate enough to represent the interactions between CO_2 molecules. The remaining differences (below 4%) between the measured values and those computed with PES2[10] and PES3[7] are probably due to the classical treatment of molecular rotations and the accuracy of the intermolecular potential used in the calculation. Furthermore, rCMDS calculations were performed at 0.2 atm only, whereas the pressure considered in the measurements is up to 1 atm (see Sec. II B and Refs. 28 and 29) hence the influence of line-mixing and neighboring lines effects may not be negligible.[29]

C. Non-Voigt effects on the line shape

In order to quantify the non-Voigt effects on the line shape, we consider the pressure dependences of the Lorentz line widths and of the fit residuals, both obtained from fits with the Voigt profile of the rCMDS-calculated spectra as well as of the measured ones. This allows a direct comparison between the *ab initio* rCMDS calculations and measurements as done in Ref. 6. In the fitting procedure, the Lorentz line width, the line position and the line integrated intensity are adjusted while the Doppler widths are fixed to the theoretical values. The potential PES3[10] is retained in this section for the comparison with the measurements.

Typical comparisons between *ab initio* rCMDS spectra and measured profiles are displayed in Fig. 4. This figure shows the residuals obtained from fits of calculated and measured spectra with Voigt profiles for two lines and various Lorentz to Doppler widths (Γ_L/Γ_D) ratios. The relative wavenumber scale is normalized by the corresponding Voigt width Γ_V, estimated following.[30] A good agreement is ob-

served for both the amplitude and the shape of the residuals. The noise observed in the calculated rCMDS spectra (red curves) is due to the limited number of the molecules considered in the calculation, as explained in Ref. 6. Within the experimental signal-to-noise ratio (about 1000), no asymmetry of the line shape could be observed, showing that the effect of the speed dependence of the collisional shift of these lines is small.

The evolution of non-Voigt effects from the nearly Doppler to the collisional regime is shown in Figs. 5 and 6. The amplitude of the residuals normalized by the peak absorption (denoted by W, maximum *minus* minimum values of residual as exemplified in Fig. 4) is plotted in Fig. 5 versus the Γ_L/Γ_D ratio. For all considered lines, W first increases

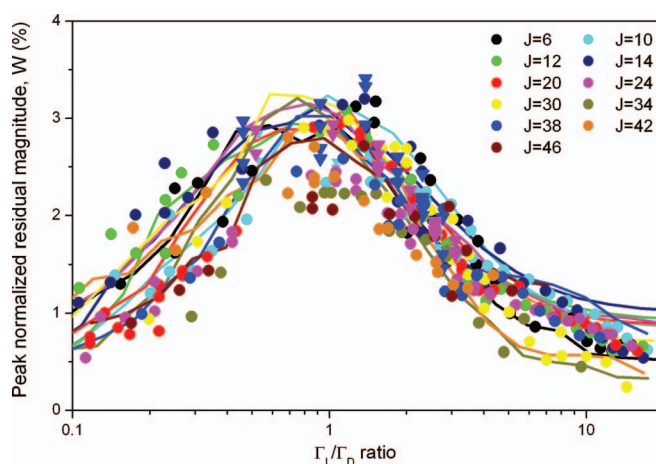

FIG. 5. Observed (symbols) and calculated (lines) amplitudes of the Voig-fit residual normalized by the peak absorption (see Fig. 4), versus the Lorentz to Doppler widths ratio. The calculated results are obtained with PES3.[10] ● are values obtained from fits with Voigt profiles of spectra measured by TDLS in the 1.6 μm region while ▼ are results obtained from CRDS spectra in the 0.8 μm region. Results for all studied lines are plotted.
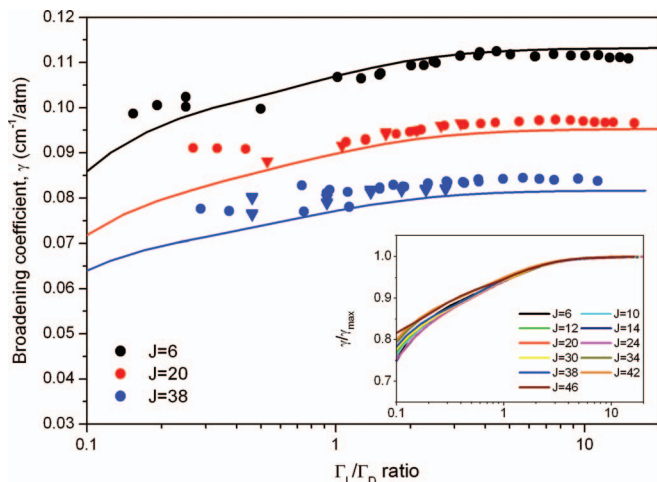
FIG. 6. Same as Fig. 5 but for the observed (● for TDLS and ▼ for CRDS measurements) and calculated (lines) Lorentz broadening coefficients, γ, for three values of the rotational quantum number J: J = 6, J = 20, and J = 38. In the inset we plot the calculated broadening coefficients of all considered lines, normalized by their maximum values (γ/γ_{max}).
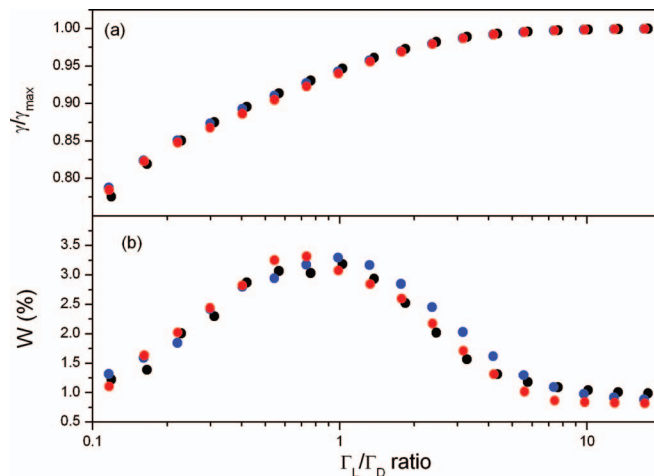

FIG. 7. Comparison between the calculated broadening coefficients (normalized by values obtained at the highest value of Γ_L/Γ_D, γ/γ_{max}) and the peak-absorption-normalized residual magnitude (W, in %) obtained with the three intermolecular potentials: PES1[9] (black), PES2[7] (red), and PES3[10] (blue). The results are for the P(10) line.

with Γ_L/Γ_D when Γ_L/Γ_D is small (the Doppler effect is dominant). It reaches a maximum (about 3%) when Γ_L is comparable to Γ_D and then decreases when Γ_L/Γ_D increases. At high value of Γ_L/Γ_D (collisional regime), W becomes constant. This evolution of W was already observed in the previous study devoted to CO_2[6] but also for other molecular systems (e.g., H_2O,[4, 31–33] O_2[34,35]). It can be explained by the relative contributions of different non-Voigt effects (velocity changes, speed-dependence of the line width and shift, correlation between velocity and internal-state changes) to the line shape in different regimes, as done in Ref. 33 for H_2O. However, such a refined analysis is beyond the scope of this paper but it will be made in a future work. The values of W deduced from rCMDS calculations are in good agreement with the experimental determinations obtained by both TDLS and CRDS in two spectral regions. As can be observed in Fig. 5, no J (i.e., line) dependence of W can be pointed out within the experimental uncertainties and the numerical noise of the rCMDS results. Note that at low and high values of Γ_L/Γ_D, W being small and then particularly affected by the numerical and experimental noises, the values of W determined from rCMDS and measured spectra have a large uncertainty ($\pm 0.5\%$).

In Figure 6 are plotted some examples of the broadening coefficients, (i.e., $\gamma = \Gamma_L/P$, with P the CO_2 pressure), obtained from fits of the rCMDS-calculated and measured spectra with Voigt profiles, for three values of the rotational quantum number: J = 6, J = 20, and J = 38. Similar results are obtained for other lines. The observed values deduced from CRDS spectra in the (10052 ← 00001) band and from TDLS spectra in the (30013 ← 00001) or (30012 ← 00001) bands are plotted together. A good agreement between the measured values in the two spectral regions is obtained, confirming that the vibrational dependence of the broadening coefficients (for these relatively low rotational quantum numbers, J $\leq$ 50) of pure CO_2 is small.[36] As observed previously,[4, 6, 31–35] the broadening coefficients increase with the Γ_L/Γ_D ratio. At high values of Γ_L/Γ_D, where only the speed dependence of

the collisional parameters contributes to non-Voigt effects on the line shape, γ becomes constant. The measured values of γ are satisfactory reproduced by the rCMDS calculations for all values of Γ_L/Γ_D and all considered lines. Some deviations can be observed at very low values of Γ_L/Γ_D where the contribution of Γ_L is very small leading to large uncertainties on the values of Γ_L fitted from measured spectra. Accurate determination of Γ_L at low Γ_L/Γ_D (low pressure) would require very high precision of the experimental set up and the pressure and temperature determinations. Similarly to the case of W, if one normalizes γ of different lines by their maximum values, all present the same evolution with Γ_L/Γ_D and no line dependence can be observed (see the insert in Fig. 6). A similar conclusion was obtained for isolated transitions of O_2.[35]

The influence of the used PES on the calculated line shape is presented in Fig. 7 where the values of W and of γ normalized by its maximum value (γ/γ_{max}), obtained from rCMDS-calculated spectra are plotted versus Γ_L/Γ_D for the P(10) line. While the calculated broadening coefficient depends on the intermolecular potential (Fig. 3), no potential dependence can be observed for its relative evolution with Γ_L/Γ_D (Fig. 7(a)). For both γ/γ_{max} and W, the three potentials lead to very similar results. This is in contrast to the case of the far infrared collision-induced absorption band where the same three interaction potentials led to very different results.[3, 11]

V. CONCLUSIONS AND FUTURE STUDIES

Pure CO_2 line shapes computed by requantized classical molecular dynamics simulations have been successfully compared to measured profiles for various ro-vibrational lines corresponding to a broad range of rotational quantum number. The results show that non-Voigt effects on the shape of CO_2 lines are independent of the lines within the present experimental and calculation uncertainties. This study together with the results obtained previously for a few lines of CO_2[6] and for O_2[34,35] confirms that rCMDS are a powerful tool for

ab initio predictions of the line shape of linear molecules. Hence, they can be used as a benchmark to test the different semi-empirical approaches which are widely used to fit measured spectra ([37] and references therein). Moreover, detailed information on the different mechanisms contributing to the line shape can also be obtained from rCMDS, such as the collision-induced velocity changes, the speed-dependent line width, and the correlation between the velocity and internal-state changes. Based on this, the influence of each non-Voigt effect contributing to the line shape can be analyzed. These will be the subjects of our future studies.

ACKNOWLEDGMENTS

[1]H. Tran, J.-M. Hartmann, F. Chaussard, and M. Gupta, J. Chem. Phys. **131**, 154303 (2009).

[2]J. M. Hartmann, C. Boulet, H. Tran, and M. T. Nguyen, J. Chem. Phys. **133**, 144313 (2010).

[3]J.-M. Hartmann, C. Boulet, and D. Jacquemart, J. Chem. Phys. **134**, 094316 (2011).

[4]N. H. Ngo, H. Tran, and R. R. Gamache, J. Chem. Phys. **136**, 154310 (2012).

[5]J.-M. Hartmann and C. Boulet, J. Chem. Phys. **134**, 184312 (2011).

[6]J.-M. Hartmann, H. Tran, N. H. Ngo, X. Landsheere, P. Chelin, Y. Lu, A.-W. Liu, S.-M. Hu, L. Gianfrani, G. Casa, A. Castrillo, M. Lepere, Q. Deliere, M. Dhyne, and L. Fissiaux, Phys. Rev. A **87**, 013403 (2013).

[7]S. Bock, E. Bich, and E. Vogel, Chem. Phys. **257**, 147 (2000).

[8]Y. Lu, A.-W. Liu, X.-F. Li, J. Wang, C.-F. Cheng, Y. R. Sun, R. Lambo, and S.-M. Hu, ApJ **775**, 71 (2013).

[9]C. S. Murthy, S. F. O'Shea, and I. R. McDonald, Mol. Phys. **50**, 531 (1983).

[10]R. Bukowski, J. Sadlej, B. Jeziorski, P. Jankowski, K. Szalewicz, S. A. Kucharski, H. L. Williams, and B. M. Rice, J. Chem. Phys. **110**, 3785 (1999).

[11]A. P. Kouzov and M. Chrysos, Phys. Rev. A **80**, 042703 (2009).

[12]N. Ibrahim, P. Chelin, J. Orphal, and Y. I. Baranov, J. Quant. Spectrosc. Radiat. Transfer **109**, 2523 (2008).

[13]N. H. Ngo, N. Ibrahim, X. Landsheere, H. Tran, P. Chelin, M. Schwell, and J. M. Hartmann, J. Quant. Spectrosc. Radiat. Transfer **113**, 870 (2012).

[14]L. S. Rothman, I. E. Gordon, A. Barbe, D. C. Benner, P. F. Bernath, M. Birk, V. Boudon, L. R. Brown, A. Campargue, J.-P. Champion, K. Chance, L. H. Coudert, V. Dana, V. M. Devi, S. Fally, J.-M. Flaud, R. R. Gamache, A. Goldman, D. Jacquemart, I. Kleiner, N. Lacome, W. J. Lafferty, J.-Y. Mandin, S. T. Massie, S. N. Mikhailenko, C. E. Miller, N. Moazzen-Ahmadi, O. V. Naumenko, A. V. Nikitin, J. Orphal, V. I. Perevalov, A. Perrin, A. Predoi-Cross, C. P. Rinsland, M. Rotger, M. Simeckova, M. A. H. Smith, K. Sung, S. A. Tashkun, J. Tennyson, R. A. Toth, A. C. Vandaele, and J. Vander Auwera, J. Quant. Spectrosc. Radiat. Transfer **110**, 533 (2009).

[15]C. F. Cheng, Y. R. Sun, H. Pan, Y. Lu, X.-F. Li, J. Wang, A.-W. Liu, and S.-M. Hu, Opt. Express **20**, 9956 (2012).

[16]J.-M. Hartmann and C. Boulet, J. Chem. Phys. **136**, 184302 (2012).

[17]T. Vieillard, F. Chaussard, F. Billard, D. Sugny, O. Faucher, S. Ivanov, J.-M. Hartmann, C. Boulet, and B. Lavorel, Phys. Rev. A **87**, 023409 (2013).

[18]J. Lamouroux, J.-M. Hartmann, H. Tran, B. Lavorel, M. Snels, S. Stefani, and G. Piccioni, J. Chem. Phys. **138**, 244310 (2013).

[19]M. P. Allen and D. J. Tildesley, *Computer Simulation of Liquids* (Clarendon, Oxford, 1987).

[20]H. Tran, C. Boulet, S. Stefani, M. Snels, and G. Piccioni, J. Quant. Spectrosc. Radiat. Transfer **112**, 925 (2011).

[21]M. S. Green, J. Chem. Phys. **20**, 1281 (1952).

[22]R. Kubo, J. Phys. Soc. Jpn. **12**, 570 (1957).

[23]E. R. S. Winter, Trans. Faraday Soc. **47**, 342 (1951).

[24]E. B. Winn, Phys. Rev. **80**, 1024 (1950).

[25]I. Amdur, J. W. Irvine, E. A. Mason, and J. Ross, J. Chem. Phys. **20**, 436 (1952).

[26]R. P. Wendt, J. N. Mundy, S. Weissman, and E. A. Mason, Phys. Fluids **6**, 572 (1963).

[27]K. Schäfer and P. Reinhard, Z. Naturforsch. A **18**, 187 (1963).

[28]R. A. Toth, L. R. Brown, C. E. Miller, V. M. Devi, and D. C. Benner, J. Mol. Spectrosc. **239**, 243 (2006).

[29]A. Predoi-Cross, A. V. Unni, W. Liu, I. Schofield, C. Holladay, A. R. W. McKellar, and D. Hurtmans, J. Mol. Spectrosc. **245**, 34 (2007).

[30]J. J. Olivero and R. L. Longbothum, J. Quant. Spectrosc. Radiat. Transfer **17**, 233 (1977).

[31]H. Tran, D. Bermejo, J.-L. Domenech, P. Joubert, R. R. Gamache, and J.-M. Hartmann, J. Quant. Spectrosc. Radiat. Transfer **108**, 126 (2007).

[32]N. H. Ngo, H. Tran, R. R. Gamache, D. Bermejo, and J.-L. Domenech, J. Chem. Phys. **137**, 064302 (2012).

[33]H. Tran, N. H. Ngo, J.-M. Hartmann, R. R. Gamache, D. Mondelain, S. Kassi, A. Campargue, L. Gianfrani, A. Castrillo, E. Fasci, and F. Rohart, J. Chem. Phys. **138**, 034302 (2013).

[34]J.-M. Hartmann, V. Sironneau, C. Boulet, T. Svensson, J. T. Hodges, and C. T. Xu, Phys. Rev. A **87**, 032510 (2013).

[35]J. Lamouroux, V. Sironneau, J. T. Hodges, and J.-M. Hartmann, "Isolated line shapes of molecular oxygen: ab initio calculations versus measurements," Phys. Rev. A (submitted).

[36]R. R. Gamache and J. Lamouroux, J. Quant. Spectrosc. Radiat. Transfer **117**, 93 (2013).

[37]N. H. Ngo, D. Lisak, H. Tran, and J.-M. Hartmann, J. Quant. Spectrosc. Radiat. Transfer **129**, 89 (2013).